

# EE568 Project 3: PM Motor Comparison Analysis

Baris Kuseyri

May 3, 2020

# Contents

|          |   |           |
|----------|---|-----------|
| <b>1</b> | <b>Introduction</b>   | <b>2</b>  |
| <b>2</b> | <b>Q1- Magnetic Loading</b>   | <b>2</b>  |
| 2.1      | Magnetic Equivalent Circuit, Magnet Load Line and Peak Air-gap Flux Density                                 | 3         |
| 2.2      | b. Magnetic Loading . . . . .   | 4         |
| 2.3      | c. FEA Results . . . . .  | 5         |
| <b>3</b> | <b>Q2- Electrical Loading &amp; Machine Sizing</b>  | <b>6</b>  |
| 3.1      | a. Number of Slots . . . . .  | 6         |
| 3.2      | b. AWG Cable . . . . .  | 6         |
| 3.3      | c. Slot Height, Number of Coils per Slot, and Back-core Thickness . . . . .                                 | 7         |
| 3.4      | d. Electrical Loading . . . . .   | 8         |
| 3.5      | e. Average Tangential Stress & Total Force . . . . .  | 8         |
| 3.6      | f. Expected Power Output . . . . .  | 9         |
| <b>4</b> | <b>Q3- Comparison &amp; Optimization</b>  | <b>9</b>  |
| 4.1      | a. Optimum Rotor Diameter . . . . .   | 9         |
| 4.2      | b. Replacing NdFeB with Ferrite . . . . .   | 10        |
| 4.3      | c. Optimizing Ferrite Machine . . . . .   | 10        |
| <b>5</b> | <b>Conclusion</b>   | <b>10</b> |
| <b>A</b> | <b>Magnetic Circuit</b>   | <b>11</b> |
| <b>B</b> | <b>Error Calculation</b>  | <b>13</b> |
| <b>C</b> | <b>Electrical Loading <math>\bar{A}</math> as a function of Rotor Radius — Constant Stator Outer Radius</b> | <b>13</b> |

## 1 Introduction

This project aims to prepare a study similar to what was done by W. L. Soong in his case study on Ferrite versus NdFeB. In his study, Soong replaces rare earth NdFeB magnets with ferrite magnets in an SPM machine. Later, he increases the thickness of the magnets and equalizes the flux density levels on stator tooth and back iron region of the machine with NdFeB magnets and ferrite magnets. Unlike Soong's study, this project sets the stator outer diameter constant [1].

First, this project designs a SPM in part 2, to analyse the magnetic loading of a machine. Then, in part 3, it determines several machine parameters. The project continues by analysing electric loading of the machine, and the resulting average tangential stress, total force, torque and power output.

The starting values are given in Table 1, below.

|                            | symbol     | unit | value |
|----------------------------|------------|------|-------|
| number of phases           | $m$        |      | 3     |
| number of pole-pairs       | $p$        |      | 2     |
| motor axial length         | $l_m$      | mm   | 100   |
| air-gap clearance          | $\delta_g$ | mm   | 1     |
| magnet to pole pitch ratio |            |      | 0.8   |
| magnet radial thickness    | $t_m$      | mm   | 4     |

Table 1: Machine Parameters

## 2 Q1- Magnetic Loading

This project starts by analysing the magnetic loading of an SPM machine. The stator is assumed to be solid for this part. Additional to the parameters given in Table 1, some extra values are set as starting values. Parameters on rare earth magnet are given in Table 2 and rotor diameter is given in Table 3.

|                       | symbol  | units | value     |
|-----------------------|---------|-------|-----------|
| magnet type           |         |       | NdFeB N42 |
| shape                 |         |       | radial    |
| relative permeability | $\mu_r$ |       | 1.05      |
| coercivity            | $H_c$   | A/m   | 994529    |

Table 2: Permanent Magnet Parameters

|                | symbol | unit | value |
|----------------|--------|------|-------|
| rotor diameter | $D_r$  | mm   | 100   |

Table 3: Rotor Dimensions

## 2.1 Magnetic Equivalent Circuit, Magnet Load Line and Peak Air-gap Flux Density

Magnetic equivalent circuit for one pole-pair is shown in Fig. 1. Here, each PM is modelled as an MMF source, meaning it's equivalent model is composed of a voltage source with a value of  $F = \phi R_m$ , and a resistance  $R_m$  connected in series.

Starting with PM #1, the flux  $\phi$  goes through the airgap, modelled as  $R_g$ , and splits into two components at the stator back iron. Each half of the flux goes through the back iron, in opposite directions. Here, only one pole-pair is shown, so only one half-of-the-flux is described further. This half flux component then merges with, again what is another half flux component, and travels through the airgap, modelled again as  $R_g$ . Then, it travels through PM #2, and splits into two. One of the components merges with another half flux components and goes through PM #1. Hence, the cycle is completed.

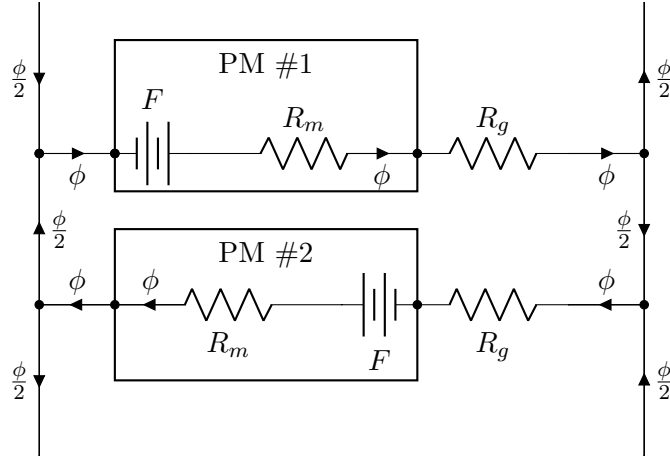


Figure 1: magnetic equivalent circuit for one pole-pair

Magnetic loading of a machine refers to the average airgap flux density over a pole. This value can be calculated by

$$\bar{B} = \frac{p\phi_p}{\pi D_r l} \quad (1)$$

where  $\bar{B}$  is specific magnetic loading,  $p$  is the number of poles,  $\phi_p$  is flux per pole,  $D_r$  is rotor diameter, and  $l$  is the axial length of the machine. Equation 1 interprets specific

magnetic loading  $\bar{B}$  as total flux going out of the rotor surface divided by total rotor surface area.

To find out  $\phi_p$ , machine's magnetic circuit is needed to be analyzed. The magnetic circuit diagram can be seen in Fig. 1.

The magnetic circuit is composed of 2 NdFeB 42 permanent magnets (PM) and 2 instances of airgaps. To analyse this circuit, PM remanence flux density  $B_r$  information is required. At this point, relative permeability  $\mu_r$  and coercivity  $H_c$  of NdFeB 42 PM is given as a part of the problem, which can be seen in Table 2. From here; remanence flux density can be found by the following relation:

$$B_r = \mu_0 \mu_r \times H_c \quad (2)$$

where,  $\mu_0$  is the permeability of air or vacuum ( $\mu_0 = 4\pi \times 10^{-7} A/m$ ). Hence, magnet remanence flux density is  $B_r = 1.31T$ . From here, peak airgap flux density  $\hat{B}_g$  is calculated via the steps stated in Appendix B. The result is  $\hat{B}_g = 1.0394T$ .

The B-H curve and the load line of the magnets in the circuit can be seen in Fig. 2. The intersection of the B-H curve and the load line presents the peak airgap flux density, which is  $\hat{B}_g = 1.0394T$  on the plot and corresponds to  $H = -205080 A/m$ .

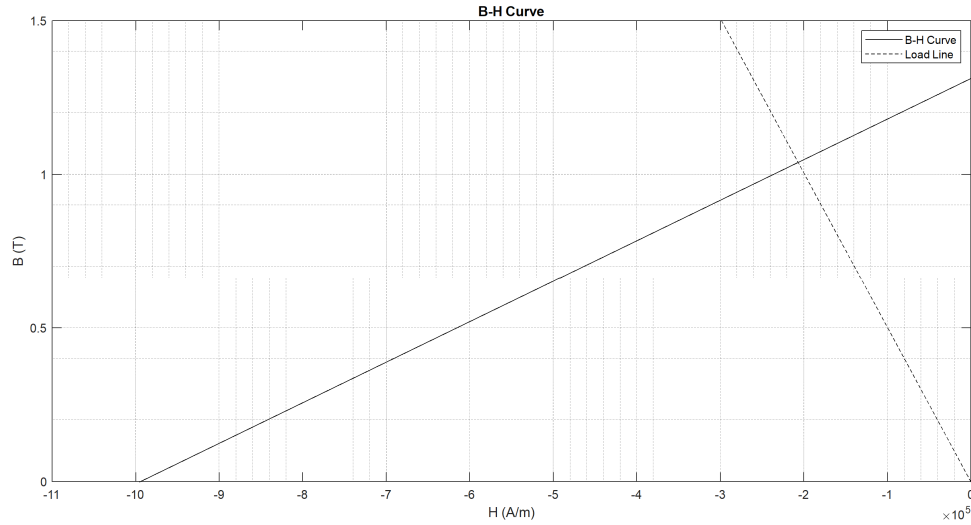


Figure 2: B-H Curve & Load Line of NdFeB Magnets

## 2.2 b. Magnetic Loading

The average airgap flux density  $B_{avg}$  corresponds to the *RMS* value of peak airgap flux density  $\hat{B}_g$ , which corresponds to specific magnetic loading  $\bar{B}$  of the machine.

$$B_{avg} = \frac{1}{\sqrt{2}} \hat{B}_g = \bar{B} \quad (3)$$

Peak airgap flux density is calculated in the previous section, and the result is  $\hat{B}_g = 1.0394T$ . Inserting this value to the Eq. 3, specific magnetic loading is  $\bar{B} = 0.7350T$ .

### 2.3 c. FEA Results

FEMM is used as FEA software. The flux density map of the machine is shown in Fig. 3. The stator is solid, meaning that there is no tooth apparent on the stator.

The airgap flux density  $B_g$  distribution can be seen in Fig. 4. The distribution peaks at a value of  $\hat{B}_g = 1.0374T$ . Specific magnetic loading is calculated by taking the average of this distribution, which results with  $B_{avg} = 0.7558T$ .

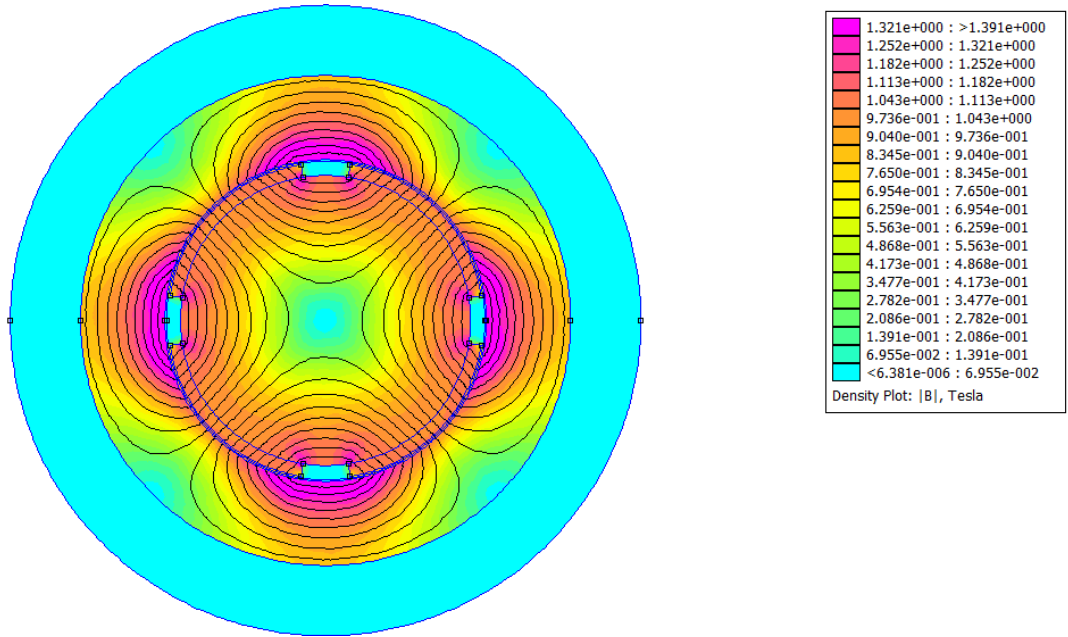


Figure 3: Flux Density Plot

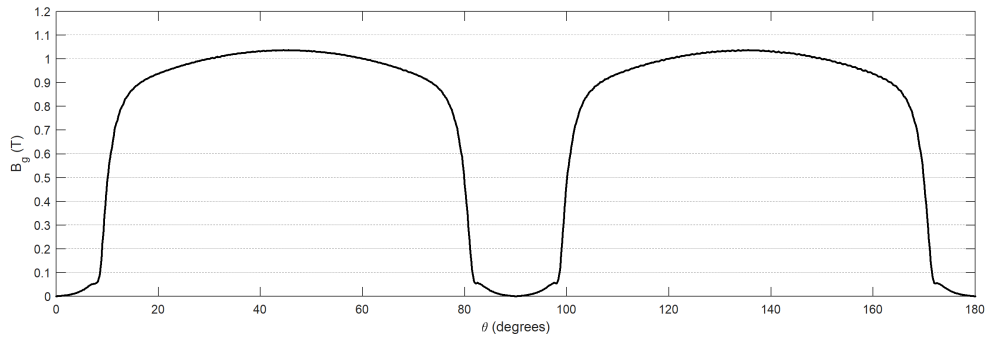


Figure 4: Airgap Flux Density Distribution

Analytical and FEA results for peak airgap flux density  $\hat{B}_g$  and magnetic loading  $\bar{B}$  are shown in Table 4.

|          | $\hat{B}_g$ | $\bar{B}$ |
|----------|-------------|-----------|
| Analytic | $1.0394T$   | $0.7350T$ |
| FEA      | $1.0374T$   | $0.7558T$ |

Table 4: Peak Airgap Flux Density and Magnetic Loading

Results obtained in pervious sections 2.2 and 2.1 comply with the results from FEA analysis. Error calculation, according to Appendix B, yields a 0.1977% error for the peak airgap flux density  $\hat{B}_g$  between the analytical and FEA results. Same calculation yields a 2.7518% error for the magnetic loading  $\bar{B}$  between the analytical and FEA results, slightly higher than it is for peak airgap flux density  $\hat{B}_g$ ; however, both error percentages are fairly small. Overall, the FEA results verify the analytical results.

### 3 Q2- Electrical Loading & Machine Sizing

#### 3.1 a. Number of Slots

This project studies machine topologies with a number of pole-pairs of  $p = 2$ . Number of slots for this machine is determined to be 12. In a 12 slot 4 pole machine, fundamental winding factor is unity, meaning the windings link all the flux components coming from the magnets. This results with no reduction of torque due to the flux linkage limitations.

Several slot numbers  $N_s$  and the corresponding winding factors  $K_w$  are given in Table 5.

| number of slots $N_s$ | winding factor $K_w$ | winding type    |
|-----------------------|----------------------|-----------------|
| 6                     | 0.866                | concentrated    |
| 9                     | 0.617                | concentrated    |
| 12                    | 1.000                | integer-slot    |
| 15                    | 0.951                | fractional-slot |
| 18                    | 0.945                | fractional-slot |

Table 5: Number of Slots and Corresponding Winding Factors

One major downside of choosing the number of slots  $N_s$  in terms to obtain a unity winding factor  $K_w$  is that there are high EMF harmonic components, which results with EMF shaping towards a trapezoidal waveform. This results with high torque ripples at the operation of the machine.

#### 3.2 b. AWG Cable

If the maximum current density  $\hat{J}$  is set to be  $5A/mm^2$  and one conductor is carrying  $2.5A$ , then the maximum number of conductors there can be in  $1mm^2$  is 2, and the total

|                      | symbol | units    | value |
|----------------------|--------|----------|-------|
| max. current density | $J$    | $A/mm^2$ | 5     |
| coil current         | $I$    | A        | 2.5   |
| fill factor          | $K_p$  |          | 0.6   |

Table 6: Current Parameters

cross-section area of 2 conductors can not be below  $1mm^2$ . Therefore, the suitable AWG cable chosen for this project is AWG 20. The characteristics of AWG20 cable can be seen in Table 7, below.

| AWG | diameter [mm] | area [mm <sup>2</sup> ] | resistance/length [mΩ/m] |
|-----|---------------|-------------------------|--------------------------|
| 20  | 0.812         | 0.518                   | 33.31                    |

Table 7: AWG 20 characteristics

As can be seen in Table 7, the cross-section area of AWG 20 cable is  $0.518mm^2$ , which corresponds to  $J = 4.83A/mm^2$ , below the maximum current density value given for this project. Using any cable with a cross-section area below  $0.500mm^2$  with a coil current of  $I = 2.5A$  would exceed this current density  $J$  limitation.

### 3.3 c. Slot Height, Number of Coils per Slot, and Back-core Thickness

This part starts by choosing a slot ratio  $d$  for the machine. This choice is done in the following fashion. Teeth shape is determined to be rectangular, slot ratio is set to be  $d = 0.6$  and tooth to slot opening ratio is assumed to be 1 to 1. Then,

$$\tau_{teeth} = \tau_{slot} = \frac{2\pi r_{si}}{2N_s} \quad (4)$$

where  $\tau_{teeth}$  is the tooth thickness and  $\tau_{slot}$  is the slot opening.

Back iron thickness is set to be 2 times the tooth thickness  $t_{backiron} = 2\tau_{teeth}$ . Thus, the back iron thickness is  $t_{backiron} = 26.7mm$ . Back iron thickness may be decreased until it is equal with tooth thickness  $\tau_{teeth}$  before it saturates. However, in machines without a strict dimensional limitations, increasing back iron thickness slightly results with a significant drop on the flux density on the back iron, resulting with much lower core losses.

$$h_t = \frac{r_{si}}{d} - r_{si} \quad (5)$$

where  $h_t$  is tooth height. Thus, tooth height is  $h_t = 34mm$ . Then, tooth area is calculated by

$$A_t = h_t \tau_{teeth} \quad (6)$$

Total slot area is equal to the annulus set by slot inner and outer radii,  $r_{si}$  and  $r_{so}$ .



$$N_s A_s = (\pi r_{so}^2 - \pi r_{si}^2) - N_s A_t \quad (7)$$

Hence, the slot area  $A_s$  is calculated.

Then, the number of conductors to be fit in a slot is determined by

$$N_{cond} = \frac{A_s K_p}{A_{cond}} \quad (8)$$

Hence, the number of conductors to be fit in one slot is  $N_{cond} = 876$ .

### 3.4 d. Electrical Loading

Now that the number of conductors per slot is determined, the electric loading of the machine can be calculated.

$$\bar{A} = \frac{1}{\sqrt{2}} \frac{N_s N_{cond} I}{2\pi r_{si}} \quad (9)$$

Eq. 45 gives the electric loading  $\bar{A} = 58000 A/m$ . This result is lower than what was stated by [2] as the maximum electric loading value for non-salient pole synchronous machines with indirect air cooling. This machine type is chosen for this comparison because the stated maximum current density  $J = 5$  corresponds to the upper limit for current density of this type of machine, again stated by [2]. Thus, the slot ratio  $d$  may be decreased.

A slot ratio of  $d = 0.545$  pushes the electric loading level to  $\bar{A} = 80000 A/m$ , which is the upper limit for the electric loading  $\bar{A}$ , stated in the book [2]. When slot ratio  $d = 0.545$ , the number of conductors to be fit in one slot is  $N_{cond} = 999$  and tooth height is  $h_t = 42.6 mm$ .

### 3.5 e. Average Tangential Stress & Total Force

The effective axial length of the machine is calculated by

$$l' = l + 2l_g \quad (10)$$

Thus, effective axial length of the machine is  $l' = 102 mm$ .

The tangential stress acting on the rotor surface  $\sigma_{tan}$  and the total tangential force acting on the rotor surface is  $F$  are calculated by

$$\sigma_{tan} = \frac{\bar{A} \hat{B}}{\sqrt{2}} \quad (11)$$

$$F = 2\sigma_{tan} \pi r_r l' \quad (12)$$

$$T = F r_r = 2\sigma_{tan} \pi r_r^2 l' \quad (13)$$

Tangential stress acting on the rotor surface is  $\sigma_{tan} = 58775 N$ , and the total tangential force acting on the rotor surface is  $F = 1883 Nm$ .

### 3.6 f. Expected Power Output

The total power output  $P$  of the machine is calculated by

$$P = T \times \omega \quad (14)$$

The total power output is  $P = 14792W$ .

## 4 Q3- Comparison & Optimization

In this part, the stator outer diameter  $D_o$  is set to be  $160mm$ , and rotor diameter  $D_r$  and other parameters are subjected to alteration. Open slot configuration and rectangular teeth geometry is determined as starting parameters.

### 4.1 a. Optimum Rotor Diameter

The aim of this part is to find the optimum rotor diameter and the slot ratio, which yields the maximum torque output. To achieve this, torque output is derived as a function of rotor radius. The derivation of electric loading as a function of rotor radius can be found in Appendix C. Then, tangential stress  $\sigma_{Ftan}$  is calculated by

$$\sigma_{Ftan} = \bar{A}\bar{B} \quad (15)$$

Here, tangential stress acting on every point on the rotor surface. Thus, integrating the tangential stress over rotor surface yields the total force  $F_{tan}$  acting on the rotor surface in the tangential direction.

$$F_{tan} = 2\sigma_{Ftan}V_r \quad (16)$$

$$= 2\sigma_{Ftan}(\pi r_{rotor,outer}^2 l_e) \quad (17)$$

To obtain the torque  $T$  equation, force  $F_{tan}$  shown in Eq. 17 is multiplied by the rotor outer radius  $r_{rotor,outer}$ .

$$T = F_{tan}r_{rotor,outer} \quad (18)$$

Thus, the relationship between rotor outer radius  $r_{rotor,outer}$  and the torque output  $T$  is set. Additionally, slot ratio  $d$  is stated as a function of rotor outer radius  $r_{rotor,outer}$ .

$$d = \frac{r_{slot,inner}}{r_{slot,outer}} \quad (19)$$

where,  $r_{slot,inner}$  and  $r_{slot,outer}$  are defined as functions of  $r_{rotor,outer}$  in Appendix C. Thus, the relationship between slot ratio  $d$  and the torque output  $T$  is set.

Using MATLAB, torque output  $T$  is plotted as a function of slot ratio  $d$ , in Fig. 5.

The torque function peaks at slot ratio  $d = 0.4313$ , with a torque value of  $T = 41.1443Nm$ .

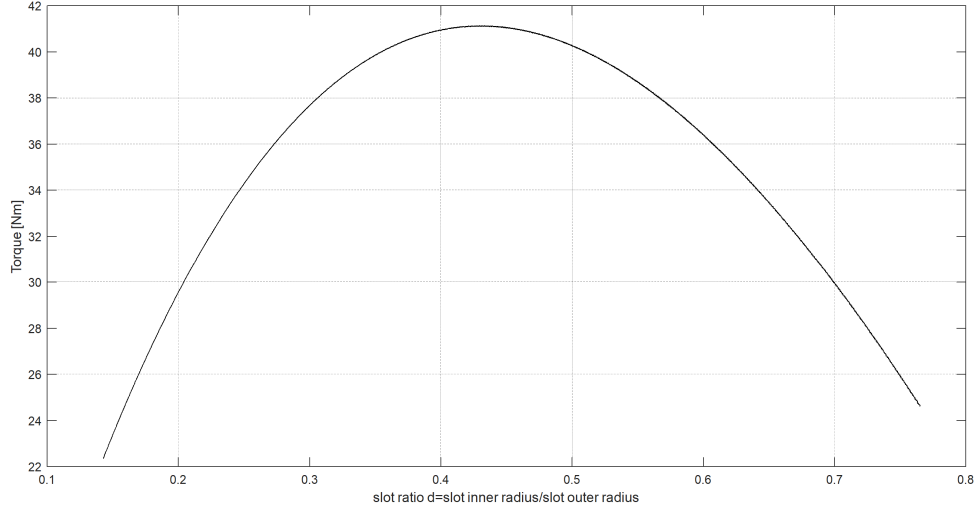


Figure 5: Torque vs. Slot Ratio

#### 4.2 b. Replacing NdFeB with Ferrite

Torque output  $T$  is plotted as a function of rotor outer radius slot ratio  $d$ , in Fig. 6.

The torque function peaks at slot ratio  $d = 0.4313$ , with a torque value of  $T = 12.5416 Nm$ . The optimum slot ratio is not different from the machine with the NdFeB magnets. However, the output torque  $T$  is decreased to 0.3 of what it is with NdFeB magnets. This is expected, while ferrite magnet remanence flux density is also 0.3 of that is of NdFeB magnets.

#### 4.3 c. Optimizing Ferrite Machine

Torque output  $T$  is plotted as a function of slot ratio  $d$  and slot-to-tooth ratio  $K_t$ , in Fig. 7. The torque function peaks at slot ratio  $d = 0.4919$  and slot-to-tooth ratio  $K_t = 0.1$ , with a torque value of  $T = 16.53 Nm$ .

Decreasing tooth width results with higher torque output. However, this is limited by mechanical constraints, while teeth are responsible for supporting the tangential stress on the rotor surface.

## 5 Conclusion

In this project, magnetic and electric loadings are analysed with a set of starting values and several assumptions based on rule of thumbs. Next, an electric machine is analysed with NdFeB magnets and Ferrite magnets. Finally, Ferrite magnet machine is optimized to be compared with the NdFeB magnet machine.

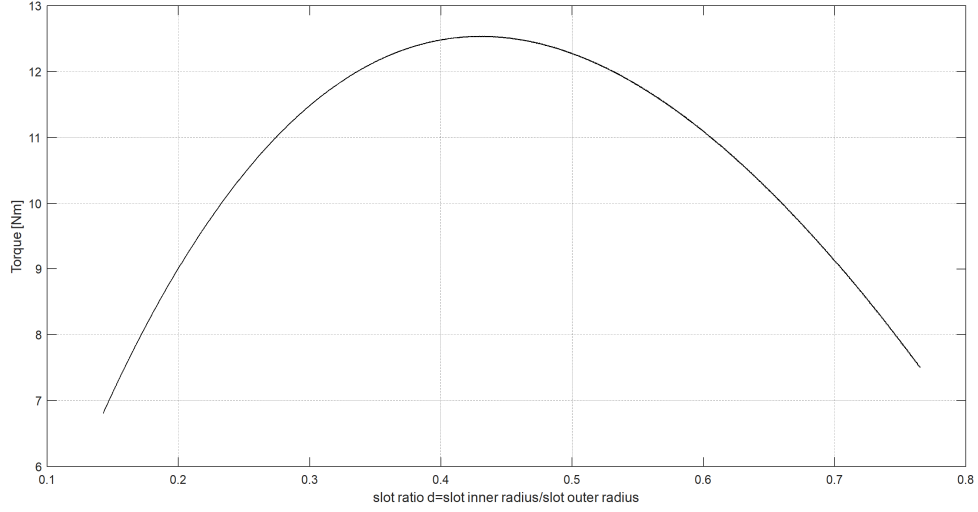


Figure 6: Torque vs. Slot Ratio

## A Magnetic Circuit

Neglecting leakage flux:

$$B_m A_m = B_g A_g \quad (20)$$

Assuming infinitely permeable core ( $\mu_c = \infty$ , where  $\mu_c$  is the core permeability)

$$H_m l_m + H_g l_g = 0 \quad (21)$$

$$H_m l_m = -H_g l_g \quad (22)$$

Now, in the airgap

$$B_g = \mu_o H_g \quad (23)$$

$$B_m A_m = \mu_o H_g A_g = -\mu_o H_m A_g \frac{l_m}{l_g} \quad (24)$$

$$\frac{B_m}{H_m} = -\frac{\mu_o A_g}{A_m} \frac{l_m}{l_g} \quad (25)$$

This is the equation of the so-called load-line of the magnetic circuit.

For a material with a linear demagnetisation characteristic:

$$B_m = B_r + \mu_o \mu_r H_m \quad (26)$$

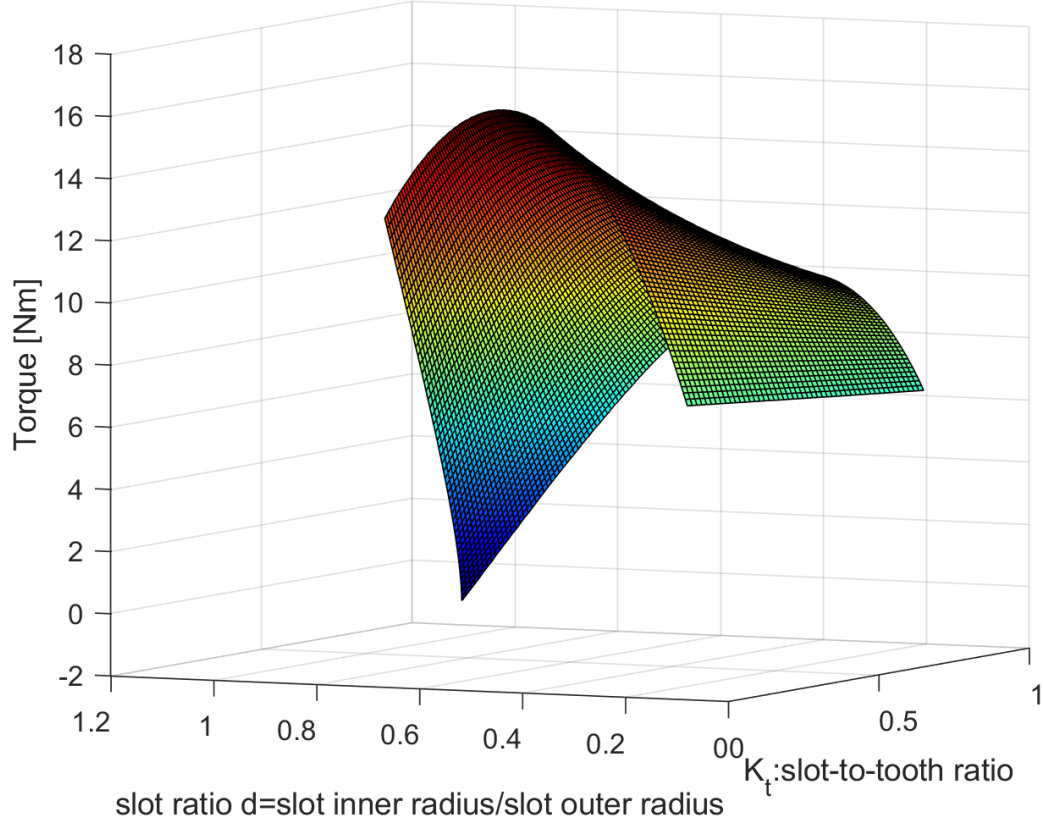


Figure 7: Torque vs. Slot Ratio vs. Slot-to-tooth Ratio

$$H_m = \frac{B_m - B_r}{\mu_0 \mu_r} \quad (27)$$

$$B_m = -\frac{A_g l_m}{A_m l_g \mu_r} (B_m - B_r) \quad (28)$$

$$B_m \left( \frac{A_g l_m}{A_m l_g \mu_r} + 1 \right) = \frac{A_g l_m}{A_m l_g \mu_r} B_r \quad (29)$$

$$B_m = \frac{\frac{A_g l_m}{A_m l_g \mu_r}}{\frac{A_g l_m}{A_m l_g \mu_r} + 1} B_r \quad (30)$$

$$B_m = \frac{B_r}{1 + \frac{A_m l_g \mu_r}{A_g l_m}} \quad (31)$$

Assuming  $A_g = A_m$ , the above equation simplifies to

$$B_g = B_m = \frac{B_r}{1 + \mu_r \frac{l_g}{l_m}} \quad (32)$$

where  $B_g$  is the airgap flux density,  $l_g$  is the airgap clearance and  $l_m$  is the magnet thickness. Here,  $B_g$  value corresponds to the peak airgap flux density  $\hat{B}_g$ .

## B Error Calculation

$$\%_{error} = \left| \frac{\#_{experimental} - \#_{theoretical}}{\#_{theoretical}} \right| * 100 \quad (33)$$

## C Electrical Loading $\bar{A}$ as a function of Rotor Radius — Constant Stator Outer Radius

To derive electrical loading  $\bar{A}$  as a function of slot inner radius, several stator dimensions are related with rotor outer radius  $r_{rotor,outer}$ .

$$r_{slot,inner} = r_{rotor,outer} + l_g \quad (34)$$

$$\tau_{teeth} = \frac{2K_t\pi r_{slot,inner}}{N_s} \quad (35)$$

$$\tau_{slot} = \frac{2(1 - K_t)\pi r_{slot,inner}}{N_s} \quad (36)$$

$$t_{backiron} = \tau_{teeth} \quad (37)$$

$$h_{slot} = r_{stator,outer} - (t_{backiron} + r_{stator,inner}) \quad (38)$$

$$r_{slot,outer} = r_{slot,inner} + h_{slot} \quad (39)$$

$$d = \frac{r_{slot,inner}}{r_{slot,outer}} \quad (40)$$

where  $r_{slot,inner}$  is the slot inner radius,  $l_g$  is the airgap clearance,  $\tau_{teeth}$  is the tooth thickness,  $K_t$  is the slot-to-tooth ratio,  $\tau_{slot}$  is the slot opening,  $t_{backiron}$  is the back iron thickness,  $h_{slot}$  is the slot height and  $r_{slot,outer}$  is the slot outer radius. Once these dimensions are set, slot area can be calculated by

$$A_{tooth} = h_{slot} \left( \frac{2\pi r_{slot,inner}}{N_s} \right) \quad (41)$$

$$A_{slot} = \frac{\pi(r_{slot,outer}^2 - r_{slot,inner}^2) - N_s A_{tooth}}{N_s} \quad (42)$$

where  $A_{tooth}$  is the tooth area and  $A_{slot}$  is the slot area. It is important to point out here that this relation assumes rectangular teeth geometry. Using the slot area  $A_{slot}$ , number of conductors is calculated by

$$N_{conductor} = \frac{K_p A_{slot}}{A_{conductor}} \quad (43)$$

where  $N_{conductor}$  is the number of conductors,  $K_p$  is the filling factor and  $A_{conductor}$  is the cross-section area of the conductors used in the machine. From this point, electric loading is calculated using the equation

$$\hat{A} = \frac{N_s N_{conductor} I}{2\pi r_{slot,inner}} \quad (44)$$

where  $\hat{A}$  is the peak linear current density. Specific electric loading  $\bar{A}$  is the RMS value of peak linear current density  $\hat{A}$ , as in Eq. 45

$$\bar{A} = \frac{1}{\sqrt{2}} \hat{A} \quad (45)$$

## References

- [1] G. Pellegrino, T. Jahns, N. Bianchi, W. Soong, and F. Cupertino, *The Rediscovery of Synchronous Reluctance and Ferrite Permanent Magnet Motors*. 01 2016.
- [2] J. Pyrhonen, T. Jokinen, and V. Hrabovcova, *Design of Rotating Electrical Machines*. Wiley, 2009.